X-ray diagnostics of runaway electrons generated during nanosecond discharge in gas at elevated pressures

S. Yatom,[a] D. Levko, J. Z. Gleizer, V. Vekselman, and Ya. E. Krasik
Physics Department, Technion, Haifa 32000, Israel

(Received 19 November 2011; accepted 14 December 2011; published online 9 January 2012)

The properties of high-energy runaway electrons generated during a nanosecond discharge in an air filled diode at pressures up to 3×10^5 Pa were studied using x-ray absorption spectroscopy. The results of studies of the discharge at different pressures and with different lengths of cathode-anode gap allow an insight into the factors that influence the energy distribution of runaway electrons. Energy distribution functions for runaway electrons produced in particle-in-cell simulation were used to create the x-ray attenuation curves via a computer-assisted technique simulating the generation of x-ray by energetic electrons. The simulated attenuation curves were compared to experimental results. © *2012 American Institute of Physics*. [doi:10.1063/1.3675462]

Nano- and sub-nanosecond timescale electrical gas discharges at elevated pressures initiated by high-voltage (HV) pulses are accompanied by the generation of high-energy (tens of keV) runaway electrons (RAE).[1] These electrons were obtained during the discharge in different types of gas and at different pressure values when applying different HV pulses with amplitudes $\geq$50 keV to cathodes having different forms.[2,3] It was supposed that RAE serve as a gas preionization source, thus being an important factor in the initiation of the discharge.[2–4] In addition, in a few experiments, sightings of "anomalous" electrons, possessing energies $E_e > e\varphi$, where φ is the amplitude of applied HV pulse, were reported.[5,6] The parameters of RAE were studied using Faraday cups, foil spectrometry, and the time-of-flight method.[1–6] Foil spectroscopy methods employing either photomultiplier tubes (PMT) or Faraday cups were used to study the dependence of parameters of the x-ray generation accompanying the discharge on pressure and voltage values[4,7] and RAE energy.[8,9] Two possible origins of RAE were proposed: field or explosive emission, from the cathode[2,3] or from the boundary of the propagating streamer. In the latter case, the streamer boundary serves as a source of RAE either continuously during streamer's propagation toward the anode[10] or only when the streamer approaches the vicinity of the anode, where the electric field becomes sufficient for RAE generation.[3]

In this paper, experimentally obtained dependencies of the attenuation of x-ray fluxes by *Al* filters (x-ray foil spectrometry) for different values of pressure, cathode-anode (CA) gap, and HV pulse parameters pulse are reported. These dependencies are compared with the results of particle-in-cell (PIC) simulations, providing insight into RAE energy spectra.

In the experiments, a gas filled diode with a CA gap of variable length (d_{CA}) was supplied by HV pulses with durations of 1, 5, and 20 ns full width at half maximum and amplitudes of ~140, ~170, and ~160 kV, respectively, produced by an all-solid state generator.[11] Typical voltage and current waveforms are shown in Fig. 1. A capacitive voltage divider and a self-integrated Rogowsky coil were used to measure the voltage and current, respectively. The cathode was made of a stainless steel blade 10 mm in length and ~3 μm in edge radius. The value of d_{CA} was changed in the range 0.5–4 cm. The anode was made of a 12.7 μm-thick *Ta* foil attached to a 2 mm-thick *Al* plate.

For x-ray spectrometry, a Saint-Gobain BC408 plastic scintillator was used with *Al* filters in front of it and a PMT Hamamatsu R7400 placed behind the filters (see Fig. 2). RAE interaction with the *Ta* foil produces x-ray bremsstrahlung radiation, which is attenuated in the *Ta* foil and *Al* filters, and induces fluorescence light emission in the plastic scintillator registered by the PMT. Thus, the time integrated signal of the PMT represents the relative amount of fluorescent photons. The time duration and amplitude of PMT signal decreases with the increase in the thickness of *Al* filters according to the x-ray energy spectrum, which in turn, depends on the RAE energy spectrum. An attenuation curve of the PMT signal versus the *Al* filter's thickness was obtained for different values of gas pressures and d_{CA}. The attenuation curves for 5 and 20 ns HV pulses and their dependence on d_{CA} and pressure are shown in Fig. 3. Here each data point represents the average of around 25 shots and the error bar does not exceed 5%. These data were normalized to the intensity behind the 2 mm-thick *Al* plate. One can see that the x-ray attenuation does not depend on the value of d_{CA} at $P = 10^5$ Pa. Let us note that the absolute value of the fluorescence light emission decreases significantly with the increase in the value of d_{CA}. The latter strongly indicates on a decrease in the amplitude of the RAE current with the

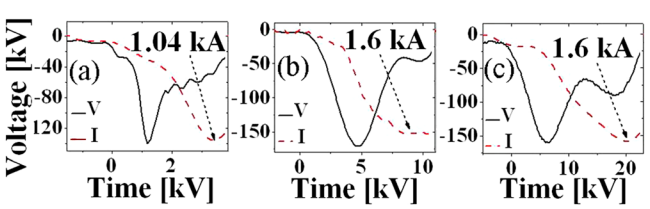

FIG. 1. (Color online) Typical voltage and current waveforms in the air-filled diode at $P = 10^5$ Pa. (a) 1 ns HV pulse, d_{CA} - 1 cm. (b) 5 ns HV pulse, d_{CA} - 1 cm. (c) 20 ns HV pulse, d_{CA} - 3 cm.

[a]Electronic mail: shurikyatom@gmail.com.

 © 2012 American Institute of Physics

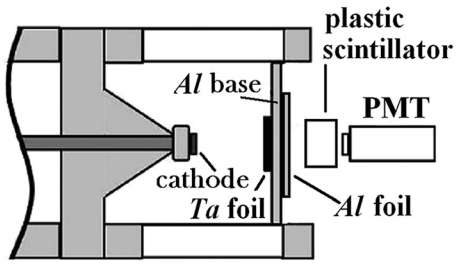

FIG. 2. Experimental setup for x-ray spectrometry.

increase in d_{CA}. The increase in d_{CA} leads to a decrease in the average electric field in the CA gap; however, this would not change significantly the potential distribution and, respectively, the electric field in the vicinity of the cathode or a front edge of the streamer. Thus one can conclude that the high energy part of the electron energy distribution function (EEDF) is mainly influenced by the non-uniform, enhanced electric field. On the other hand, one can see in Figs. 3(c) and 3(d) that an increase in gas pressure leads to faster decay of the x-rays versus the thickness of *Al* filters for a fixed CA gap. Also, the absolute amplitude of the light emission decreases with an increase in pressure for a fixed value of the CA gap and *Al* filter thickness. Thus, one can conclude that an increase in the pressure leads to a decrease in the amplitude of RAE current and the high-energy part of the EEDF.

In order to simulate RAE generation in N_2, a one-dimensional (1D) PIC code[12] was used. A coaxial diode was considered, with the cathode and the anode having radii of 3 μm and 1 cm, respectively. The simulation was carried out for the voltage $\varphi_C = \varphi_0 \cdot \sin(2\pi t/T)$, where $\varphi_0 = 140$ kV/160 kV/170 kV and corresponding half period times $T/2$ of 1, 5, and 10 ns. The simulation was used to obtain EEDF for various values of pressure and a CA gap of 1 cm. These EEDF were used as input parameters for the PC simulations described in detail in Ref. 13 for producing x-ray attenuation curves, which were compared with experimental data. These simulations included the electron energy losses in the *Ta* foil using the data on electron stopping power,[14] and the generation of x-rays is calculated using the forward bremsstrahlung cross-section.[15] The decay of the simulated x-ray spectrum in the *Ta* foil and *Al* filters was calculated using the x-ray attenuation coefficients.[16] Taking into account x-ray energy losses in the vinyl-toluene scintillator,[16] the time integrated flux of these photons behind the *Ta* and *Al* filter was obtained for the different thicknesses of *Al* filter used in the experiment, creating a simulated attenuation curve. Several PIC-simulated EEDFs are shown at Fig. 4, with a comparison between the experimental and simulated attenuation curve for given EEDF in the insert. A good agreement between the calculated and experimentally obtained x-ray decay curves indicates the validity of the simulated EEDF.

The results showed that EEDF is not affected by a decrease in the average electric field in the discharge gap. This allows one to state that RAE acquire significant energy in the vicinity of the whisker of the cathode or at the front of the streamer where the electric field is highly non-uniform and enhanced and not decidedly affected by a decrease in the average electric field. One can suppose that earlier in the discharge the main generation of RAE probably takes place in the vicinity of the cathode and cathode micro protrusions. It has been shown[17] that in discharges sustained by HV pulses with duration of several nanoseconds, RAE with energies of tens of keV arrive at the anode after the resistive plasma channel has crossed the CA gap. Further, the discharge transfers to the low-impedance stage, during which dense highly conductive plasma channel propagates from the cathode to the anode. This plasma channel may have a streamer head with a radius on micron scale[18] with an enhanced electric field at its front. Taking into account that propagation of this

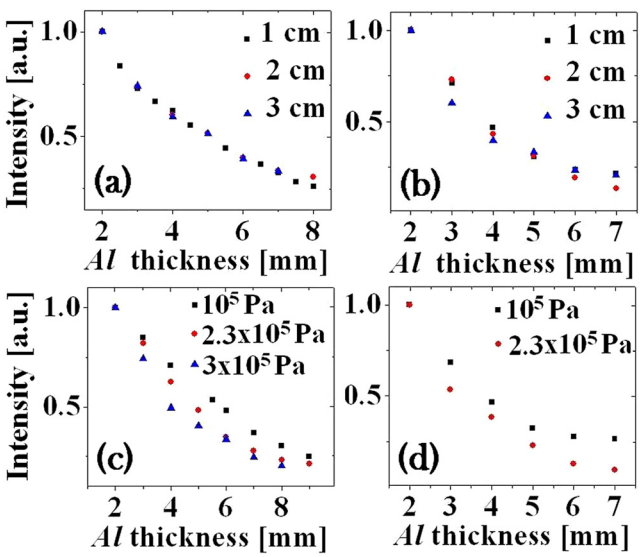

FIG. 3. (Color online) (a) 5 ns HV pulse, decay curves for $P = 10^5$ Pa and $d_{CA} = 1$, 2, 3 cm. (b) 20 ns HV pulse, decay curves for $P = 10^5$ Pa and $d_{CA} = 1$, 2, 3 cm. (c) 5 ns HV pulse, decay curves for $d_{CA} = 1$ cm and $P = 10^5$, 2.33×10^5 and 3×10^5 Pa (d) 20 ns HV pulse, decay curves for $d_{CA} = 1$ cm and $P = 10^5$ and 2.33×10^5 Pa.

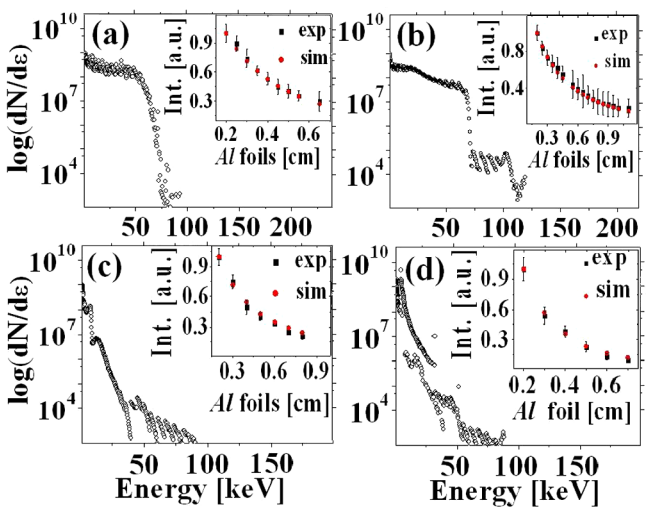

FIG. 4. (Color online) PIC simulated EEDFs, for different pressures and $d_{CA} = 1$ cm. In the insert: comparison of simulated and experimental x-ray attenuation curves. (a) HV pulse with half period of 1 ns, $P = 10^5$ Pa (b) HV pulse with half period of 2.5 ns, $P = 10^5$ Pa. (c) HV pulse with half period of 2.5 ns, $P = 3 \times 10^5$ Pa. (d) HV pulse with half period of 8 ns, $P = 2.33 \times 10^5$ Pa.

plasma leads also to a decrease in the effective CA gap and, respectively, to an increase in the average electric field, one can suppose that high-energy RAE are emitted from the front of this streamer. An increase in pressure does, however, affect the x-ray decay curves, leading to an increase in electron collisional frequency and, respectively, to a decrease in the average energy of electrons propagating toward the anode.

This work was partly supported by Lady Davis foundation.

[1]P. Babich, T. V. Loiko, V. A. Tsukerman, Soviet Phys. Usp. **33**, 521 (1990).
[2]A. Mesyats and M. I. Yalandin, IEEE Trans. Plasma Sci. **37**(6), 785 (2009).
[3]F. Tarasenko and S. I. Yakovlenko, Plasma Devices Opt. **13**, 231 (2005).
[4]T. Shao, Ch. Zhang, Zh. Niu, P. Yan, V. F. Tarasenko, E. Kh. Baksht, A. G. Burahenko, and Y. V. Shut'ko, Appl. Phys. Lett. **98**, 021503 (2011).
[5]P. Babich and T. V. Loiko, Plasma Phys. Rep. **36**, 263 (2010).
[6]V. F. Tarasenko, Plasma Phys. Rep. **37**, 409 (2011).
[7]H. G. Krompholz, L. L. Hatfield, A. A. Neuber, K. P. Kohl, J. E. Chaparro, and H. U. Ryu, IEEE Trans. Plasma Sci. **34**(3), 927 (2006).
[8]S. A. Shunailov, G. A. Mesyatz, A. G. Reutova, and M. I. Yalandin, in Proceedings 3rd Euro-Asian Pulsed Power Conference and 18th International Conference on High-Power Particle Beams, Jeju, Korea, 10–14 October 2010, Report No. 015_MoB2-2.
[9]A. V. Kozyrev, V. Yu. Kozhevnikov, E. Kh. Baksht, A. G. Buranchenko, and V. F. Tarasenko, Russ. Phys. J. **53**, 4 (2010).
[10]E. V. Oreshkin, S. A. Barenholtz, A. V. Oginov, V. I. Oreshkin, S. A. Chaikovski, and K. V. Shpakov, Lett. JTF **37**, 12 (2011).
[11]S. N. Rukin, Instrum. Exp. Tech. **42**, 439 (1999).
[12]D. Levko, S. Yatom, V. Vekselman, J. Z. Gleizer, V. Tz. Gurovitch, and Ya. E. Krasik, "Numerical simulations of runaway electron generation in pressurized gases," J. Appl. Phys. (to be published).
[13]S. Yatom, V. Vekselman, J. Z. Gleizer, V. Tz. Gurovitch, and Ya. E. Krasik, J. Appl. Phys. **109**, 073312 (2011).
[14]M. J. Berger, J. S. Coursey, M. A. Zucker, and J. Chang, "Stopping-power and range tables for electrons, protons and Helium ions," NIST Physical Reference Data.
[15]G. E. Desorby and A. L. Boyer, Med. Phys. **18**, 497 (1990).
[16]J. H. Hubbel and S. M. Seltzer, "Tables of x-ray mass attenuation coefficients and mass energy-absorption coefficients from 1 keV to 20 MeV for elements Z = 1 to 92 and 48 additional substances of dosimetric interest," NIST Physical Reference Data.
[17]S. Yatom, J. Z. Gleizer, D. Levko, V. Vekselman, V. Tz. Gurovich, E. Hupf, Y. Hadas, and Ya. E. Krasik, Europhys. Lett. **96**, 65001 (2011).
[18]Yu. P. Raizer, *Gas Discharge Physics* (Springer, Berlin, 1997), pp. 334–337.